Clim Dyn (2018) 50:1975–1992
DOI 10.1007/s00382-017-3731-9

Multi-site precipitation downscaling using a stochastic weather generator

Jie Chen[1] · Hua Chen[1] · Shenglian Guo[1]

Received: 19 November 2016 / Accepted: 4 May 2017 / Published online: 13 May 2017

Abstract Statistical downscaling is an efficient way to solve the spatiotemporal mismatch between climate model outputs and the data requirements of hydrological models. However, the most commonly-used downscaling method only produces climate change scenarios for a specific site or watershed average, which is unable to drive distributed hydrological models to study the spatial variability of climate change impacts. By coupling a single-site downscaling method and a multi-site weather generator, this study proposes a multi-site downscaling approach for hydrological climate change impact studies. Multi-site downscaling is done in two stages. The first stage involves spatially downscaling climate model-simulated monthly precipitation from grid scale to a specific site using a quantile mapping method, and the second stage involves the temporal disaggregating of monthly precipitation to daily values by adjusting the parameters of a multi-site weather generator. The inter-station correlation is specifically considered using a distribution-free approach along with an iterative algorithm. The performance of the downscaling approach is illustrated using a 10-station watershed as an example. The precipitation time series derived from the National Centers for Environment Prediction (NCEP) reanalysis dataset is used as the climate model simulation. The precipitation time series of each station is divided into 30 odd years for calibration and 29 even years for validation. Several metrics, including the frequencies of wet and dry spells and statistics of the daily, monthly and annual precipitation are used as criteria to evaluate the multi-site downscaling approach. The results show that the frequencies of wet and dry spells are well reproduced for all stations. In addition, the multi-site downscaling approach performs well with respect to reproducing precipitation statistics, especially at monthly and annual timescales. The remaining biases mainly result from the non-stationarity of NCEP precipitation. Overall, the proposed approach is efficient for generating multi-site climate change scenarios that can be used to investigate the spatial variability of climate change impacts on hydrology.

Keywords Statistical downscaling · Weather generator · Inter-station correlation · Climate change impacts

1 Introduction

The assessment of climate change impacts on hydrology mainly relies on climate change information provided by global climate models (GCMs). However, the spatial resolution of GCM outputs is too coarse to be used directly for many hydrological climate change impact studies, especially over small- and meso-scale watersheds. GCMs generally provide climate change information at the grid box scale with a spatial resolution of hundreds of kilometers, while hydrological models usually require climate data at a watershed or site-specific scale. In addition, GCM outputs are subject to considerable biases, which further hinder their use as direct inputs to hydrological models for impact studies. Both dynamical and statistical downscaling approaches are used to bridge the gap between climate model outputs and the data requirements of hydrological models. Dynamical downscaling nests a regional climate model (RCM) within a GCM output field by using GCM

✉ Jie Chen
jiechen@whu.edu.cn

[1] State Key Laboratory of Water Resources and Hydropower Engineering Science, Wuhan University, 299 Bayi Road, Wuchang Distinct, Wuhan, Hubei 430072, China

initial and boundary conditions to achieve higher resolution (Dickinson et al. 1989; Giorgi 1990; Yang et al. 2010). Even though RCMs can provide climate change information at a spatial resolution of tens of kilometers, their biases inherited from GCMs still prevent their use as the direct inputs to hydrological models for most studies. For example, RCMs generally underestimate heavy precipitation and overestimate the wet-day frequency of precipitation (Guo and Senior 2006; Semenov 2007; Rosenberg et al. 2010; Herrera et al. 2010; Maraun et al. 2010; Themeßl et al. 2010; van Roosmalen et al. 2010). In addition, even though the resolution of RCMs is greatly improved, it still cannot be used for site-specific climate change impact studies. Thus, statistical downscaling is still required before using RCM simulations. Moreover, compared to GCMs, the ensemble of an RCM is still too small for investigating the uncertainty of climate change impacts, especially for less-developed regions.

Statistical downscaling is one of the techniques that link the state of some variables representing a large scale (predictors) to the states of other variables representing a much smaller scale (predictands). Compared to dynamical downscaling, statistical downscaling is computationally cheaper and much easier to apply (Wilby et al. 2002a; Zhang 2005a). The most common statistical downscaling approaches can be classified into three categories (Maraun et al. 2010): perfect prognosis (PP), model output statistics (MOS) and stochastic weather generator (WG).

PP is one of the most widely used methods, which involves estimating the statistical relationship (e.g. linear or nonlinear) between GCM predictors and local or site-specific precipitation (or other climate variables). The performance of the PP method relies on the strong relationships between predictors and predictands. Previous studies (e.g. Chen et al. 2012a, 2014a) have shown that there is usually no strong relationship between local precipitation (occurrence and amount) and large-scale climate predictors.

The MOS approach involves estimating a statistical relationship between a climate model variable (e.g. precipitation) and the same variable of the observations to correct the climate model outputs. The MOS method was first developed to correct the bias of RCM outputs, and has been applied to GCM outputs over the past few years (e.g. Chen et al. 2016). Several MOS methods, ranging from mean-based scaling to quantile mapping, have been developed and used in climate change impact studies (Ines and Hansen 2006; Christensen et al. 2008; Mpelasoka and Chiew 2009; Piani et al. 2010; Themeßl et al. 2012; Johnson and Sharma 2012; Chen et al. 2011a, 2013a; Teutschbein and Seibert 2012). Evaluation of MOS methods has shown that almost all methods are capable of reducing the biases of climate model outputs to a certain extent. In particular, quantile mapping methods generally perform better than mean-based scaling methods (Teutschbein and Seibert 2012; Chen et al. 2013b). A superior bias correction method can not only correct the magnitude of precipitation amounts, but also the wet-day frequency of precipitation occurrence. However, none of these bias correction methods are capable of correcting the temporal structure (wet and dry spells) of daily precipitation occurrence (Chen et al. 2013b), which may result in biased hydrological simulation, especially in dry seasons.

The WG method has been used as a downscaling tool for many climate change impact studies (Wilks 1992, 1999, 2010; Wilby et al. 2002b; Zhang 2005a; Qian et al. 2005, 2010; Chen et al. 2012b) since Wilks's (1992) seminal paper. Downscaling using the WG method involves adjusting WG parameters based on future climate changes projected by climate models. Downscaling WG parameters makes it possible to produce climate scenario ensembles for studying the impacts of risk-based climate events.

The single-site weather generator (SSWG) downscaling method, however, can only produce climate change scenarios at a single point (or watershed average), or independently at several points. Therefore, it is incapable of investigating the spatial variability of climate change impacts on hydrology by driving a distributed hydrological model. In particular, the convective precipitation which usually results in flood may be linked to a very localized portion of a watershed (Smith et al. 2005; Huang et al. 2012). The use of a single-site or watershed-averaged climate change scenario for an entire watershed may result in biased hydrological impacts, especially for large watersheds with complicated topographies. Multi-site weather generators (MSWG) can generate climate variables dependently for multiple sites over a watershed. During the last few decades, several MSWGs, such as the geospatial-temporal WG of Baigorria and Jones (2010), the two-stage WG of Li (2013) and the MSWG of the École de Technologie Supérieure (MulGETS) (Chen et al. 2014b), have been developed. Among the MSWGs, Wilks' (1998) model (the predecessor of MulGETS) is the one most widely studied. This model extends the commonly used SSWG by driving it with temporally-independent but spatially correlated random numbers. Several studies have focused on improving this WG approach. In particular, Chen et al. (2014b) coded the approach and streamlined it into the current form of MulGETS. Even though MSWGs have the ability to generate multi-site climate change scenarios, the literature on using MSWGs for climate change impact studies is very sparse, due to the inherent difficulties in adjusting the MSWG parameters.

Using MulGETS as a basis, this study proposes a method for simultaneously downscaling precipitation for multiple locations within a watershed. The proposed approach can be considered as a hybrid method combining

a quantile mapping method with a MSWG. The quantile mapping method is used to spatially downscale climate model-simulated monthly precipitation from a grid scale to a site-specific scale. The downscaled monthly precipitation is then disaggregated into daily data by adjusting the MulGETS parameters.

2 Study area and data

2.1 Study area

Since the importance of generating multi-site climate change scenarios is more significant for large watersheds than for small ones, a large watershed (Hanjiang River watershed) located in south-central China is used as an example to illustrate the multi-site downscaling approach (Fig. 1). The Hanjiang River watershed is one of the largest tributaries of the Yangtze River. The Hanjiang River originates from the south side of the Qinling Mountains and joins the Yangtze River in the city of Wuhan. The Hanjiang River watershed is composed of several tributaries draining a surface of approximately 159,000 km^2. The catchment above the Danjiangkou reservoir, with a surface area of 89,540 km^2, is used in this study. The Danjiangkou reservoir serves as a water source for the middle route of the South-to-North Water Diversion Project. The watershed has a subtropical monsoon climate with a mean annual precipitation of about 840 mm. Most precipitation occurs between April and October, resulting in high flows over this period, whereas the remainder of the year has little precipitation and much lower flows. The average maximum and minimum temperature between 1961 and 2000 were 19.8° and 10.0 °C, respectively. The daily mean discharge of the Hanjiang River is about 1150 m^3/s. The quantification of climate change impacts on hydrology using high-quality climate change scenarios is an important factor in water resource management for the Hanjiang River watershed.

2.2 Data

This study uses both observed and the National Centers for Environment Prediction (NCEP) reanalysis (Kalnay et al. 1996) precipitation. The observed daily precipitation is derived from ten meteorological stations dispersed across the Hanjiang River watershed above the Danjiangkou reservoir (Fig. 1). The NCEP precipitation is used as a climate model simulation to present and test the multi-site downscaling approach. The observed and the NCEP precipitation covers the period during 1957–2015. In order to reduce the risk of the model being over-fitted to a period affected by the interannual variability of the climate system, the 59-year time period is separated into 30 odd years for calibration and 29 even years for validation. This split-sample cross-validation approach is commonly used in climate change and hydrology studies. When using this multi-site downscaling method, only monthly NCEP precipitation is required. The resolution of NCEP precipitation data is 1.9° × 1.875° latitude and longitude. When using NCEP precipitation, the four nearest neighbouring grid points are interpolated to the target station using an inverse distance weighting method. For point scale climate change impact

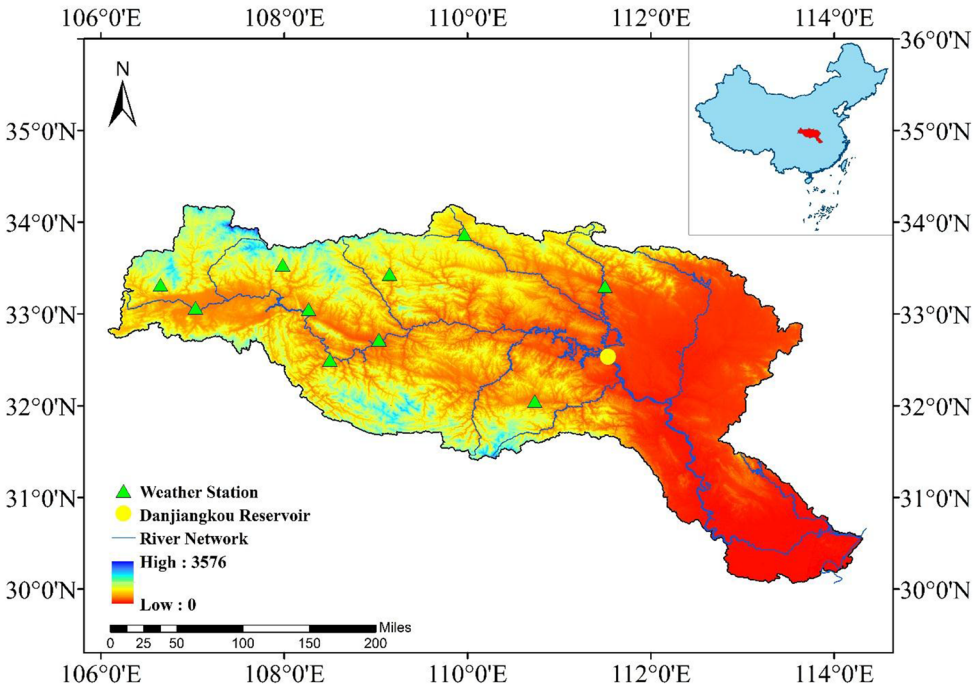

Fig. 1 Location map of the Hanjiang River watershed

studies, a minimum of four grid boxes is normally used to avoid the danger of non-representative data (Li et al. 2011; Zhang et al. 2011).

3 Methodology

The multi-site downscaling approach has two stages. The first stage spatially downscales the monthly precipitation from the NCEP scale to station scale using a quantile mapping method. The second stage disaggregates the downscaled monthly precipitation to daily values using a MSWG. The disaggregation involves adjusting MulGETS parameters using climate information derived from the downscaled monthly precipitation. Prior to presenting the two-stage downscaling approach in detail, MulGETS is briefly described below. More details can be found in Chen et al. (2014b).

3.1 Multi-site weather generator of the École de Technologie Supérieure (MulGETS)

MulGETS simultaneously generates daily precipitation, maximum and minimum temperatures for multiple sites. Precipitation is generated independently of temperature. Only precipitation generation is presented here. MulGETS is an extension of an SSWG made by driving the single-site model by temporally-dependent and spatially-correlated random numbers. The spatially-correlated random number field is generated using the distribution-free approach of Iman and Conover (1982). This approach has been used in several studies to induce inter-station and inter-variable corrections. For example, Zhang (2005b) and Chen et al. (2009) used this method to induce desired rank correlation between precipitation amounts and durations. More details about this method can be found in Chen et al. (2014b). However, when using the distribution-free approach to induce targeted inter-station correlations, the correlation of a random series must be higher than that of the precipitation occurrence (and amounts), but how much higher is initially unknown. To obtain the target correlation, an iterative algorithm was proposed by Brissette et al. (2007) to optimize the random series correlation.

Based on spatially-correlated random number fields, MulGETS generates precipitation similarly to most parametric SSWGs (e.g. WGEN of Richardson (1981) and WeaGETS of Chen et al. (2012c)). Specifically, the precipitation occurrence is generated using a first-order, two-state Markov chain, and precipitation amounts are generated using a probability distribution. When using a first-order Markov chain, the probability of precipitation on a given day (t) is based on the precipitation status (wet or dry) of the previous day, which is defined in terms of two transition probabilities: P01 and P11.

$$P01 = P\{precip.\ on\ day\ t \mid no\ precip.\ on\ day\ t-1\} \quad (1a)$$

$$P11 = P\{precip.\ on\ day\ t \mid precip.\ on\ day\ t-1\} \quad (1a)$$

If a random number drawn from a uniform distribution for a given day is less than the precipitation probability for the previous day, a precipitation event is determined.

For the determined wet day, the precipitation amount is generated using a multi-exponential distribution (Brissette et al. 2007). A multi-distribution is used rather than a single distribution, because the iterative algorithm-generated correlation matrices may fail to converge for generating precipitation amounts. For example, the correlation of precipitation amounts generated using two identical random number series between two nearby stations may still be less than that of the observed data for small watersheds with a large number of stations (Chen et al. 2014b). Wilks (1998) called this problem "spatial intermittence". To solve it, Brissette et al. (2007) proposed an occurrence index (OI) to link the mean precipitation amounts to the occurrence at the watershed scale. The OI (K) for a station m is calculated with the following equation.

$$K_m = OC^T / UC^T \quad (2)$$

where O is the occurrence vector for every station except station m, C is a vector containing the correlation between the occurrence at station m and every other station, C^T is the transpose of C, and U is a unit vector with the same length as vector C. The correlation vector C is used as a weighting scheme reflecting the fact that the behaviour of the closest neighbour is more important than that of a distant neighbour.

Figure 2 shows an example of the relationship between the OI and the daily mean precipitation for the July precipitation at all 10 stations. A strong relationship between the OI and the daily mean precipitation is observed for all stations. An exponential distribution is fitted for precipitation amounts corresponding to each OI to form a multi-exponential distribution for each station and each month. For example, five exponential distributions are fitted for the July precipitation at the first station in Fig. 2, since there are five OI values. Specifically, for this case, the daily precipitation is classified into five groups based on OI. An exponential distribution is then fitted for each group to form a 5-exponential distribution. Mathematically, the form of the multi-exponential distribution is given below.

$$D(x) = \sum_{i=1}^{n} \alpha_i \left(1 - e^{-\lambda_i x}\right) \quad with \quad \sum_{i=1}^{n} \alpha_i = 1 \quad (3)$$

The multi-exponential distribution parameters are defined based on the fitted curves of the OI, as shown

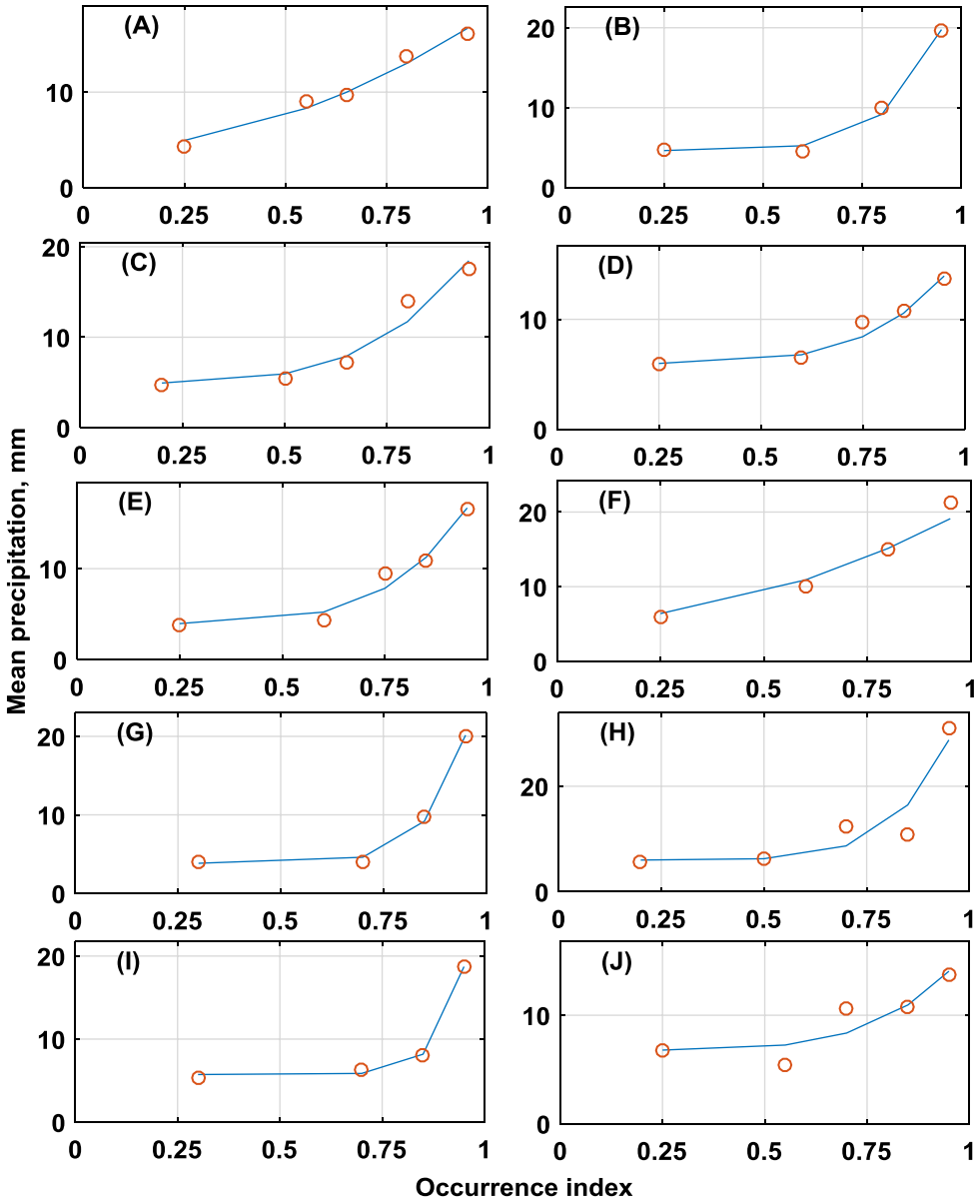

Fig. 2 Relationship between daily mean precipitation and the occurrence index for July precipitation

in Fig. 2. In Eq. (3), x is the daily precipitation, n is the number of the OI (the number of classes), α_i is the ratio of the number of precipitation events in each class to the total number of events, and λ_i is the parameter of each exponential distribution, which is the inverse of the mean precipitation for each class. Ever though the single exponential distribution has been found to be less than ideal with respect to simulating daily precipitation, especially extreme precipitation events (Chen and Brissette 2014a, b), the multi-exponential distribution performed reasonably well (Brissette et al. 2007; Chen et al. 2014b, 2015a), as it specifically considers extreme precipitation events using an exponential distribution. MulGETS also provides the option of using multi-gamma distribution to generate daily precipitation, while little advantage was observed when using a more complicated distribution (Chen et al. 2014b, 2015a).

3.2 Two-stage downscaling method

A quantile mapping method is first used to spatially downscale monthly precipitation from NCEP grid scale to point scale. Each station is downscaled individually with no consideration of the multi-site correlation. This quantile mapping was originally proposed by Zhang (2005a) and subsequently used for several impact studies (e.g. Li et al. 2011; Chen et al. 2014c; Mullan et al. 2016). One of the advantages of this method is that it only requires monthly climate change projections. Generally, monthly climate simulations are more reliable and readily

available than daily simulations (Maurer and Hidalgo 2008). When using this quantile mapping method, the observed and the NCEP monthly precipitation is first sorted in ascending order for each month of the calibration period. The first- and third-order polynomials are then fitted between the ranked station-observed and NCEP monthly precipitation for each month of the calibration period. In the last step, the established polynomials are applied to NCEP monthly precipitation for the validation period. The third-order polynomial is used for monthly precipitation values that are within the range in which the third-order polynomial is fitted, since it always shows better performance than the first-order polynomial for the calibration period. For the out-of-range values, the first-order polynomial is used to generate conservative approximations. For example, if the NCEP monthly precipitation ranges between 10 mm and 100 mm for the calibration period, to obtain monthly precipitation over the validation period, all values within this range [10–100] are downscaled using the third-order polynomial, while all values larger 100 or smaller than 10 are downscaled using the first-order polynomial. More details of this quantile mapping method can be found in Zhang (2005) and in Chen et al. (2014c). After the spatial downscaling, the mean and variance of monthly precipitation are calculated for each station and each month of the validation period for the second stage of temporal downscaling.

Temporal downscaling involves adjusting the MulGETS's precipitation parameters. Downscaling of precipitation occurrence is achieved by adjusting three probabilities: two conditional transition probabilities (P01 and P11) and one unconditional probability (π) for each station. The unconditional probability of precipitation occurrence is the independent chance that a wet or dry status occurs in the whole time series, and can be expressed as:

$$\boldsymbol{\pi} = \frac{P_{01}}{1 + P_{01} - P_{11}} \tag{4}$$

Adjusting precipitation occurrence probabilities is based on a four-point linear regression method, which involves establishing the relationships between the probabilities and monthly precipitation for each month (Zhang et al. 2012; Chen et al. 2014c). For each month of the calibration period, the observed daily precipitation is first divided into dry and wet groups according to the monthly total precipitation. To achieve this, the monthly total precipitation is first calculated based on the observed daily precipitation time series for each specific month and each station. For each month, the 30 monthly precipitation values are then sorted with an ascending order. The first 15 years are defined as the dry group and the second 15 years are defined as the wet group. Finally, the observed daily precipitation corresponding to the monthly precipitation of each group are pooled together for calculating P01, P11,π and the mean monthly precipitations (R_m). For example, 465 values (31 days $\times$ 15 years) are used to calculate the above four parameters for January. Two sets of parameters are calculated for the two groups. In addition, the 30-year observed daily precipitation is also divided into two equal sub-periods (15 years for each period), and P01, P11, π and R_m are then calculated for each sub-period. Two additional sets of parameters are calculated for these two sub-periods. In total, four sets of parameters are computed. A linear relationship is fitted between P01 (P11 or π) and R_m using the four data points for each month and each station. The separation of wet and dry groups is to insure that the fitted relationship is applicable to non-stationary climate conditions and the separation of two even groups is to include additional data points in between to fit a more reliable linear relationship. Previous studies (e.g. Zhang et al. 2012; Zhang 2013) showed that the four points' regression can improve the estimate of P01 and P11 slightly better than the two endpoints' interpolation. For the validation period, the two parameters among P11, P01 and π with the largest coefficient of determination are obtained by using the fitted linear equations and the spatially-downscaled R_m. The remaining single parameter is then calculated using Eq. (4).

Downscaling precipitation amounts involves adjusting the OI curve (e.g. Fig. 2) for each month. The adjusted OI curve is obtained by multiplying the change of daily precipitation between the calibration and the validation periods by the OI curve at the calibration period for each month. When using this method, all mean precipitation corresponding to different OIs is assumed to have the same change. In the real world, heavy and low precipitation events may change differently. It is not an easy task to estimate the relationship between the change and the magnitude of daily precipitation. To obtain the change in daily precipitation between the calibration and validation periods, the mean daily precipitation should first be calculated for the validation period. The mean daily precipitation (u_d) for the validation period is calculated using the spatially-downscaled mean monthly precipitation (u_m) and π, as shown in Eq. (5).

$$\mu_d = \frac{\mu_m}{N_d \pi} \tag{5}$$

where N_d is the number of days in a month and $N_d\,\pi$ is the average number of wet days in a month.

If the multi-gamma distribution is used to simulate daily precipitation, the daily precipitation variance must also be adjusted. As with mean daily precipitation, the adjustment of daily precipitation variance involves adjusting the

OI curves of the relationship between the OI and the precipitation variance using changes in the precipitation variance between the calibration and validation periods. The daily variance (σ_d^2) for the validation period can be obtained using Eq. (6), based on the variance of spatially-downscaled monthly precipitation (σ_m^2).

$$\sigma_d^2 = \frac{\sigma_m^2}{N_d \pi} - \frac{(1-\pi)(1+r)}{1-r}\mu_d^2 \tag{6}$$

where r is a dependence parameter that is equal to the difference between P11 and P01 (P11–P01). The parameters of gamma distribution are easy to calculate based on their relationship to mean daily precipitation and variance.

All of the adjusted parameters including P01, P11 and the OI curves for all 12 months and all 10 stations are input to MulGETS to generate 100 years of daily precipitation for the validation period. It should be noted that there is no adjustment in inter-station correlation coefficients. In other words, the inter-station correlation is assumed to be constant over time. For climate change impact studies, the inter-station correlation is assumed to be constant between historical and future periods. To prove this assumption, Fig. 3a, b present the correlation coefficients of precipitation occurrence and daily precipitation amount, respectively, during the calibration period versus those of the validation period. The results of all 12 months and 10 stations are pooled together, totalling 540 points ($C_{10}^2 \times 12$) in each graph. Figure 3a, b show that the assumption of constant inter-station correlations is generally valid for test periods. However, the separation of odd and even years implies that precipitation between calibration and validation periods is stationary. In order to verify this assumption in non-stationary precipitation conditions, 10 continuous years with the highest annual precipitation amounts (areal precipitation over 10 stations) and the other continuous 10 years with lowest annual precipitation amounts are extracted from the 59-year historical records. The mean annual precipitation of the first 10 years is 24% more than that of the second 10 years [(highest-lowest)/lowest], which represents a potential wet condition in the future. In contrast, the mean annual precipitation of the second 10 years is 19% less than that of the first 10 years [(lowest–highest)/highest], which represents a potential dry condition in the future. The inter-station correlation coefficients are calculated for both periods. Figure 3c, d present the correlation coefficients of the wet condition versus those of the dry condition for precipitation occurrence and daily precipitation amounts, respectively. As with Fig. 3a, b, 540 points are plotted in Fig. 3c, d. The results show that data points are distributed around the 1:1 line, which indicates that the constant assumption of the inter-station correlation is still valid for non-stationary precipitation conditions.

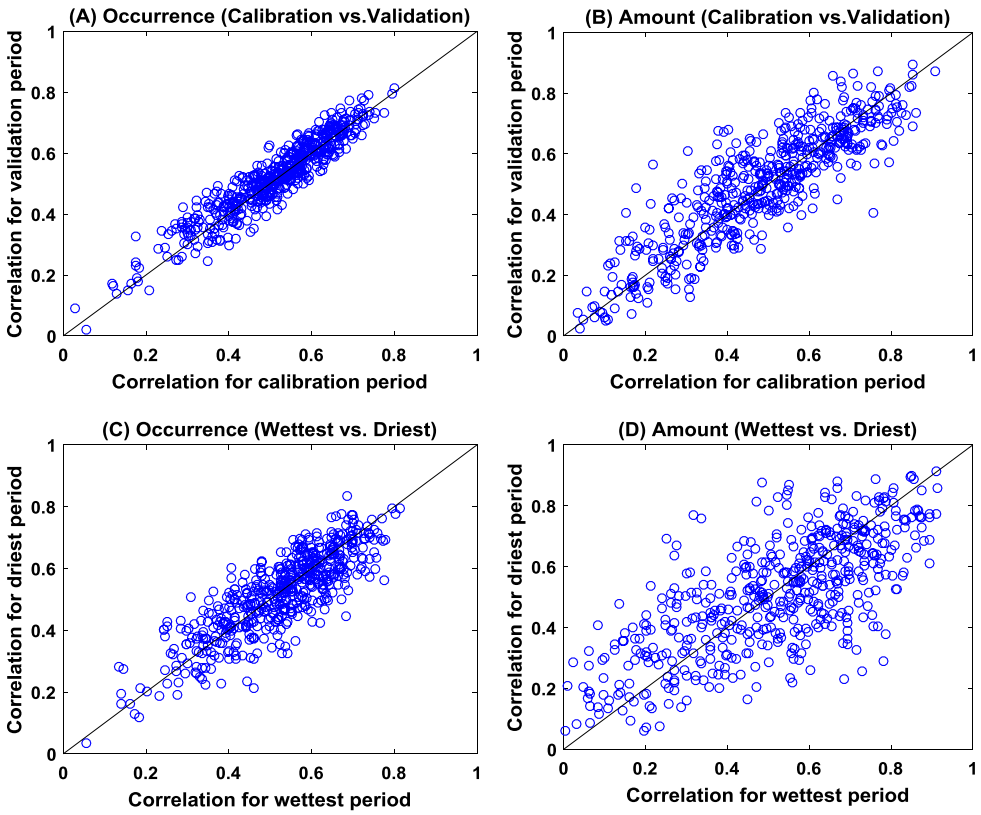

Fig. 3 Correlation relationships between calibration and validation periods and between 10-year wettest and driest periods for both precipitation occurrence (**a, c**) and daily precipitation amounts (**b, d**)

3.3 Data analysis

The NCEP monthly precipitation is downscaled to daily values for all stations within the Hanjiang River watershed. The results of the calibration process are analyzed first. The spatial downscaling performance is indicated using QQ-plots (Figs. 4, 5). The relationship between mean monthly precipitation and three probabilities of precipitation occurrence is also presented. The observed inter-station correlations versus generated correlations are plotted for both precipitation occurrence and amounts to show the performance of MulGETS with respect to preserving inter-station correlation.

To further verify the performance of the multi-site downscaling method, the downscaled daily precipitation is compared to the observed precipitation using the frequency of wet and dry day spells and the statistics of daily, monthly and annual precipitation as criteria. The precipitation statistics include the mean, standard deviation, skewness and kurtosis coefficients and the different percentiles representing the precipitation distribution. In addition, a nonparametric K–S test, applicable to any type of distribution, was used to test the agreement between the two population distributions of observed versus downscaled monthly and annual precipitation data.

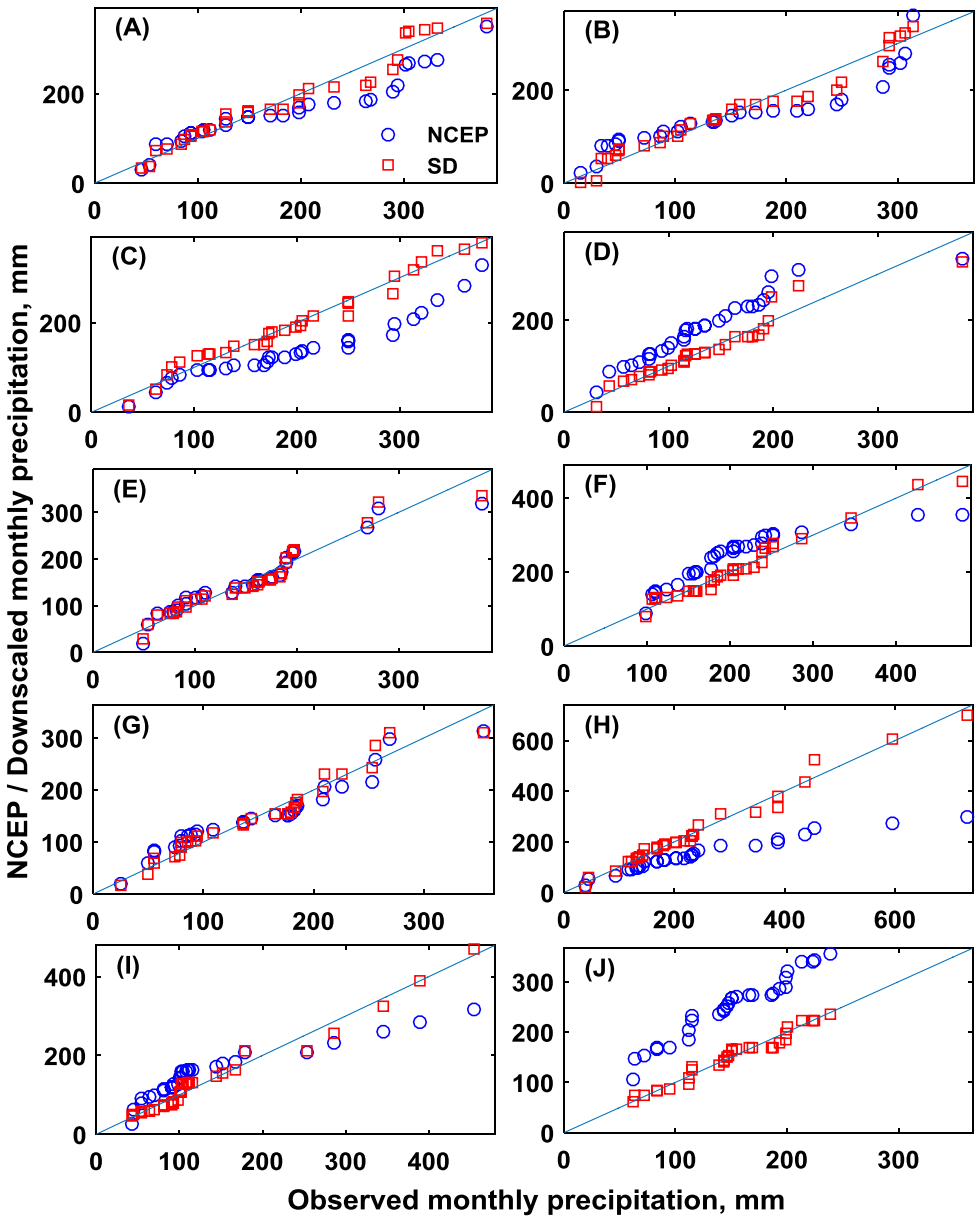

Fig. 4 QQ-plots of the station-observed monthly precipitation versus the NCEP and spatially downscaled (SD) monthly precipitation for the calibration period. Only the July results are presented. *Letters* **a**–**j** represent ten different stations within the Hanjiang River watershed

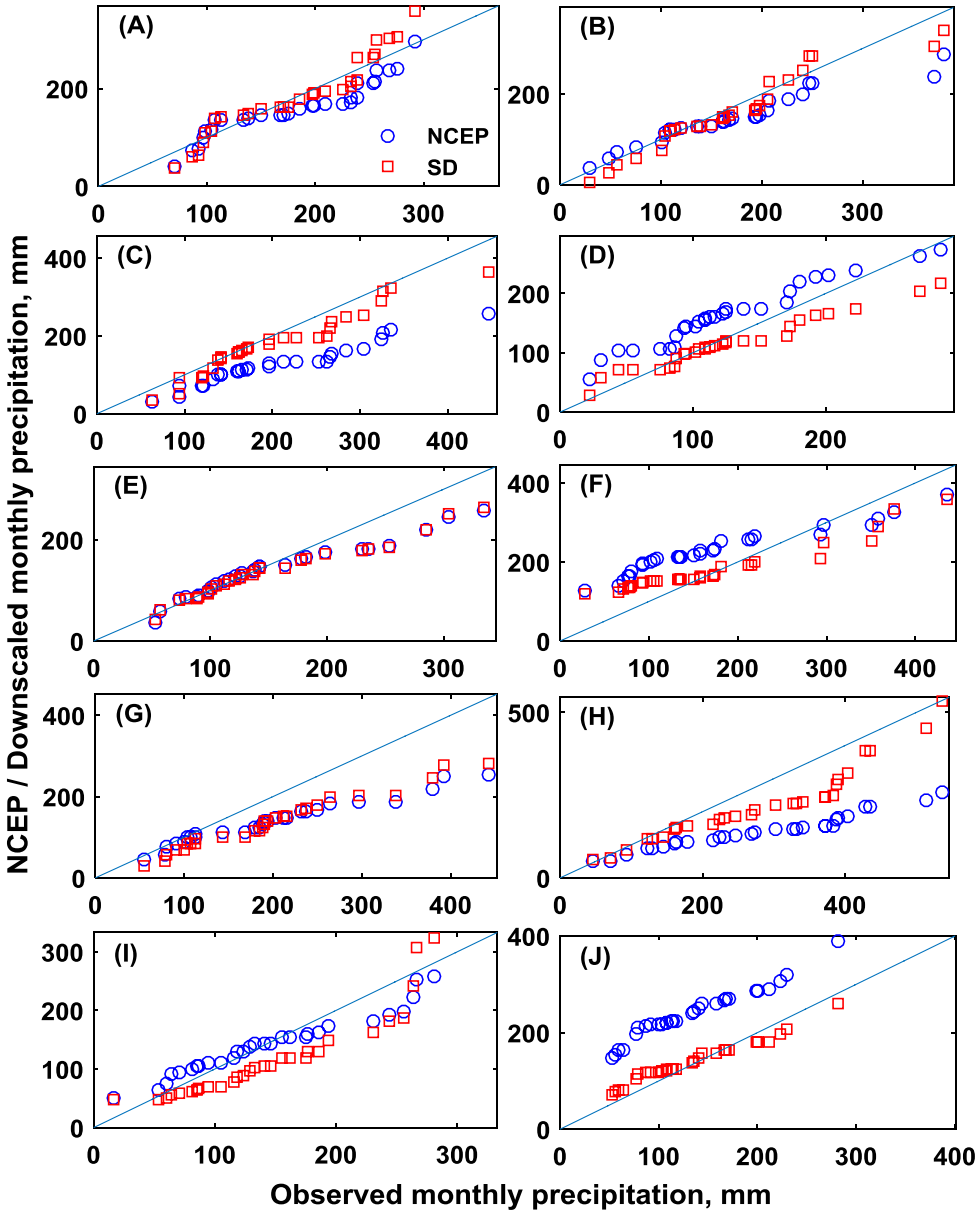

Fig. 5 QQ-plots of station-observed monthly precipitation versus the NCEP and spatially downscaled (SD) monthly precipitation for the validation period. Only the July results are presented. *Letters* **a**–**j** represent ten different stations within the Hanjiang River watershed

4 Results

4.1 Model calibration

4.1.1 Spatial downscaling

Table 1 shows the R^2 of polynomials fitted between the observed and the NCEP monthly precipitation for all months and stations over the calibration period. Generally, the fitted curves reproduce the probability distribution of observed monthly precipitation very well. The third-order polynomial consistently performs better than the first-order, as indicated by the monthly mean R^2 values ranging between 0.96 and 0.97 for the former and between 0.86 and 0.92 for the latter.

Figures 4 and 5 present the QQ-plots of the July precipitation amounts of all ten stations for the calibration and validation periods, respectively. Since similar results are obtained for all months, only the July results are presented as an illustration. The results show that the NCEP reanalysis reasonably reproduces the July precipitation for two (E and G) out of the ten stations, as indicated by the data points, which are close to the 1:1 line (Fig. 4). However, the NCEP reanalysis underestimates the July precipitation for two stations (C and H), and overestimates the July precipitation for three stations (D, F and J) to various degrees. For the other three stations, low precipitation is generally overestimated, while high precipitation is underestimated. Figure 4 also shows the QQ-plots for the downscaled July precipitation of the

Table 1 Determination coefficients of first- and third-order polynomials between station-observed and NCEP monthly precipitation for the calibration period for all 10 stations within the Hanjiang River watershed

Source	Station	Jan	Feb	Mar	Apr	May	Jun	Jul	Aug	Sep	Oct	Nov	Dec	Mean
Non-linear	S1	0.98	0.96	0.98	0.96	0.98	0.98	0.95	0.90	0.98	0.97	0.96	0.97	0.96
	S2	0.96	0.90	0.99	0.98	0.96	0.96	0.95	0.96	0.98	0.99	0.96	0.97	0.96
	S3	0.98	0.99	0.99	0.98	0.98	0.95	0.97	0.95	0.99	0.98	0.94	0.98	0.97
	S4	0.98	0.97	0.96	0.95	0.97	0.96	0.92	0.94	0.97	0.98	0.98	0.94	0.96
	S5	0.99	0.96	0.98	0.94	0.98	0.97	0.94	0.90	0.98	0.97	0.98	0.98	0.96
	S6	0.98	0.97	0.97	0.99	0.98	0.98	0.97	0.99	0.98	0.97	0.94	0.98	0.97
	S7	0.92	0.96	0.97	0.96	0.95	0.98	0.95	0.94	0.98	0.97	0.97	0.98	0.96
	S8	0.95	0.96	0.98	0.98	0.97	0.95	0.98	0.96	0.99	0.93	0.98	0.97	0.97
	S9	0.95	0.98	0.98	0.97	0.98	0.96	0.97	0.97	0.98	0.97	0.98	0.97	0.97
	S10	0.96	0.97	0.98	0.97	0.96	0.97	0.96	0.97	0.99	0.98	0.97	0.99	0.97
Linear	S1	0.96	0.95	0.95	0.96	0.89	0.93	0.92	0.84	0.95	0.84	0.93	0.97	0.92
	S2	0.77	0.85	0.88	0.97	0.91	0.84	0.85	0.96	0.94	0.76	0.81	0.96	0.88
	S3	0.79	0.98	0.70	0.83	0.84	0.95	0.92	0.92	0.96	0.85	0.81	0.93	0.87
	S4	0.90	0.93	0.81	0.76	0.90	0.90	0.87	0.93	0.94	0.86	0.91	0.93	0.89
	S5	0.97	0.88	0.59	0.77	0.88	0.90	0.93	0.89	0.94	0.85	0.92	0.97	0.88
	S6	0.97	0.94	0.95	0.80	0.88	0.98	0.73	0.91	0.91	0.71	0.92	0.90	0.88
	S7	0.78	0.96	0.71	0.71	0.89	0.97	0.93	0.90	0.97	0.59	0.94	0.95	0.86
	S8	0.92	0.96	0.88	0.80	0.84	0.87	0.94	0.94	0.98	0.90	0.98	0.93	0.91
	S9	0.79	0.96	0.85	0.58	0.87	0.92	0.85	0.95	0.97	0.76	0.92	0.97	0.87
	S10	0.70	0.94	0.91	0.52	0.72	0.94	0.95	0.97	0.84	0.96	0.95	0.90	0.86

calibration period using the quantile mapping method for all 10 stations, indicating the performance of the quantile mapping method at reproducing the probability distribution of the station-observed monthly precipitation. The results show that the probability distribution of observed monthly precipitation is well-reproduced, regardless of the behaviour of the NCEP precipitation.

Generally, the quantile mapping method satisfactorily downscales the NCEP monthly precipitation to a target station for the validation period (Fig. 5). For the two cases that the NCEP monthly precipitation is well-reproduced for the calibration period, the quantile mapping method does not alter the probability distribution of NCEP monthly precipitation for the validation period. It should be noted that the behaviour of NCEP reanalysis may be different between the calibration and validation periods. In this case, the quantile mapping method is incapable of reducing the difference. For example, NCEP reasonably reproduces the monthly precipitation for station *G* over the calibration period, while underestimates it over the validation period. In such cases, the quantile mapping method will still preserve the probability distribution of the NCEP precipitation. For all other stations, the quantile mapping method forces the NCEP monthly precipitation to be close to the observed monthly precipitation. In other words, the quantile mapping method is capable of reducing the difference between station-observed and NCEP precipitation time series. However, since the magnitude of underestimation or overestimation is not exactly the same between the calibration and the validation periods, the quantile mapping performance deteriorates slightly for the validation period.

4.1.2 Temporal downscaling

The precipitation occurrence is downscaled by linking the three probabilities of precipitation occurrence (P11, P01 and π) to mean monthly precipitation. Figure 6 presents the four points' linear regression curves for the calibration period, and three probabilities of the validation period for July precipitation at each of the 10 stations. The P11, P01 and π probabilities show a linear increasing trend of the mean monthly precipitation for all stations. In addition, the probabilities are generally well reproduced for the validation period for all stations, which indicates the reliability of fitted linear curves.

The correlations between mean monthly precipitation and three probabilities of precipitation occurrence for all 12 months' pooled data (n = 4 points × 12 months = 48) are calculated for all ten stations. Table 2 shows the Pearson correlation coefficient for three probabilities for all ten stations. Generally, there is a strong correlation between probabilities' of precipitation occurrence and mean monthly precipitation, as indicated by the values of the correlation coefficients all being greater than 0.7. The correlation between P01 (and π) and mean monthly precipitation is stronger than that between P11 and mean monthly precipitation for 7 of the 10 stations. This is consistent with the results of previous studies conducted in

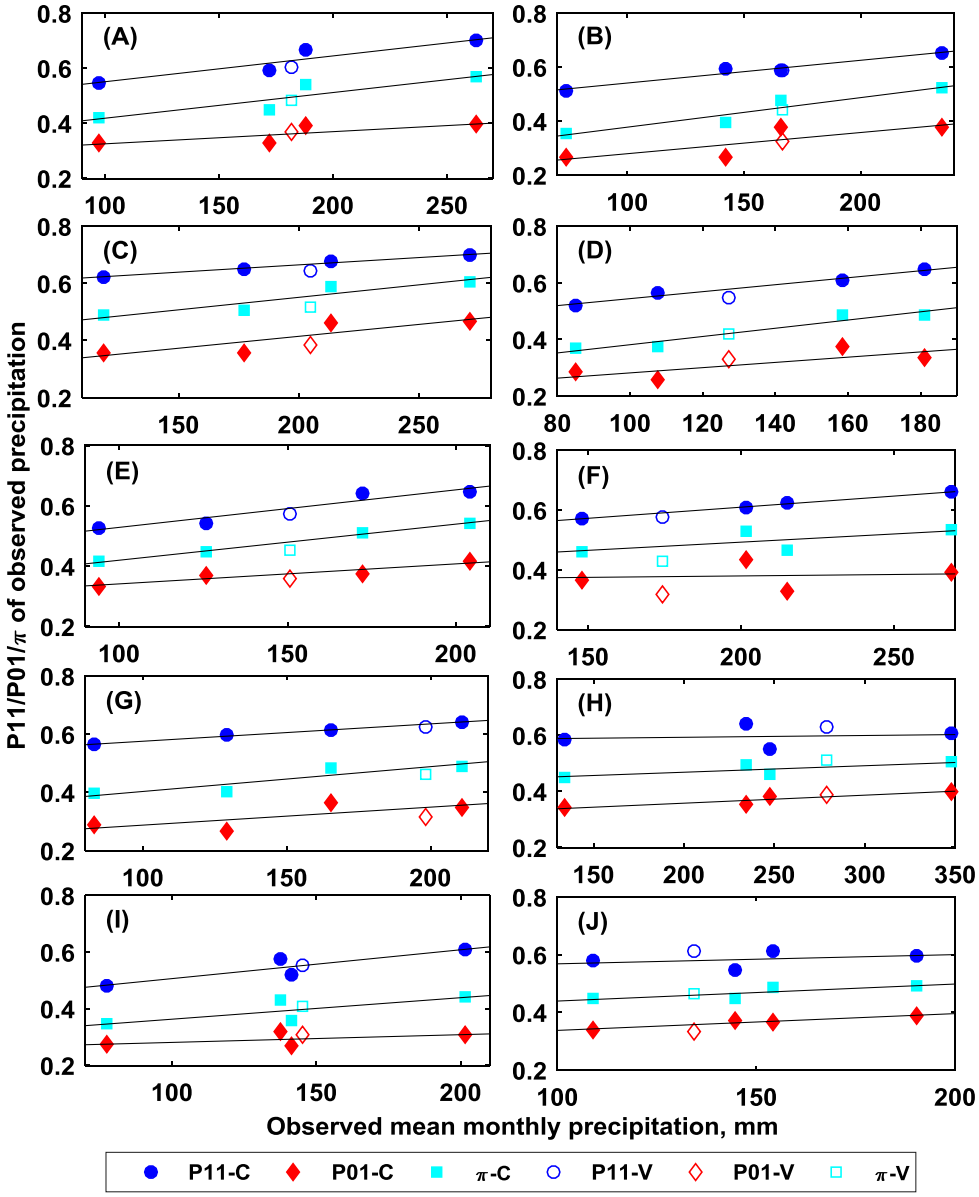

Fig. 6 Relationships between mean monthly precipitation (July) and probabilities of precipitation occurrence (P11, P01 and π) for both the calibration (C) and validation (V) periods. The *straight line* is the four points' linear regression

Table 2 Pearson's correlation coefficients between the mean monthly precipitation and the probabilities of precipitation occurrence (P11, P01 and π) for all 12 months (n = 48) for all ten stations within the Hanjiang River watershed

Source	S1	S2	S3	S4	S5	S6	S7	S8	S9	S10	Mean
P11	0.82	0.77	0.80	0.77	0.75	0.76	0.81	0.80	0.81	0.77	0.79
P01	0.86	0.85	0.88	0.88	0.89	0.89	0.80	0.74	0.76	0.89	0.84
π	0.88	0.88	0.91	0.92	0.91	0.91	0.86	0.83	0.84	0.89	0.88

other regions (Zhang 2013; Zhang et al. 2012; Chen et al. 2014c). Thus, P11 was calculated based on P01 and π for these stations by manipulating Eq. (4).

4.1.3 Inter-station correlation

The main advantage of downscaling MSWG parameters rather than using SSWG is to preserve the inter-station correlation of climate variables. These inter-station

correlations allow the generated climate change scenarios to be used to drive a distributed hydrological model for assessing the spatial variability of climate change impacts on hydrology. Figure 7 presents scatter plots of the observed inter-station correlations of precipitation occurrence and amounts versus their downscaled counterparts for all station pairs. All of the data points from 12 months and ten stations are pooled together, totalling 120 data points for each scatter plot. The scatter plots show that the inter-station correlation is well reproduced for both precipitation occurrence and amounts for all 12 months and all ten stations. This is as expected, as the iterative algorithm in MulGETS forces generated correlations to be close to observed correlations.

4.2 Downscaling verification

4.2.1 Precipitation occurrence

Figure 8 illustrates the frequencies of dry and wet spells of precipitation occurrence for the validation period for all ten stations. The performance of the downscaling method in reproducing the distribution of dry and wet spells depends on the accuracy of the temporally-downscaled probabilities of precipitation occurrence (Fig. 6). Figure 8 shows that the cumulative frequencies of observed wet and dry spells are accurately reproduced for all months and stations, illustrated by the fact that the observed and downscaled cumulative frequencies overlap each other in the figure.

4.2.2 Precipitation amount

The statistics of the downscaled daily precipitation amounts are compared with those of the observed data for the validation period over all ten stations (Table 3). The mean daily precipitation is generally well-reproduced. The standard deviation of daily precipitation is underestimated for all stations. This is partly because WG usually underestimates the high frequency of precipitation. The skewness and the kurtosis coefficients of daily precipitation amounts are poorly reproduced by the multi-site downscaling method for most stations. The downscaling method overestimates the percentiles of light and median precipitation (25th and 50th) for most stations, while it underestimates the percentiles of heavy precipitation for all stations. The maximum daily precipitation (MDP) is underestimated for 7 out of 10 stations, and overestimated for the other 3 stations. The mean of wet days per year is well reproduced for most stations, with absolute relative errors ranging between 1.87 and 6.43%, further indicating its reasonable performance in downscaling precipitation occurrence.

Compared to daily precipitation, the monthly and annual precipitation is better reproduced for all stations (Tables 4, 5). Even though the mean daily precipitation is slightly underestimated, the mean monthly and annual precipitation is well reproduced with the absolute relative error, ranging between 0.23 and 9.70%. The standard deviations of monthly and annual precipitation are both underestimated, with relative errors of between −5.13 and −19.57% for monthly precipitation and between −5.39 and −32.25% for annual precipitation. The underestimation of the standard deviation of monthly and annual precipitation by WGs has been reported in many studies (e.g. Dubrovsky et al. 2004; Wang and Nathan 2007; Chen et al. 2010, 2011b), as the low-frequency component of climate variability is not taken into account by stochastic models. The skewness and the kurtosis coefficients of monthly and annual precipitation are well reproduced for most stations. In addition, the downscaling method underestimates the distributions of monthly and annual precipitation represented by different

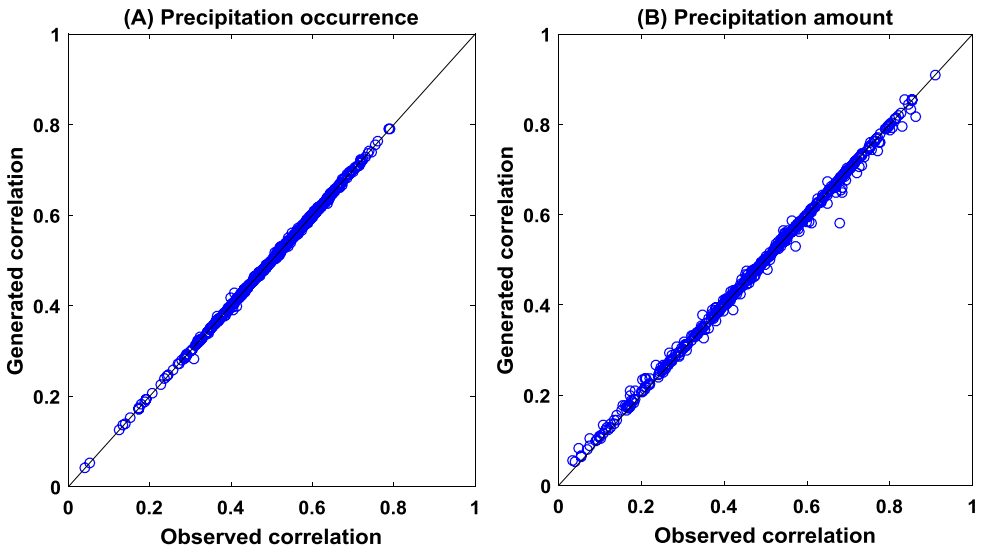

Fig. 7 Observed correlations of precipitation occurrence (**a**) and amounts (**b**) versus generated correlations for all 12 months and ten stations within the Hanjiang River watershed

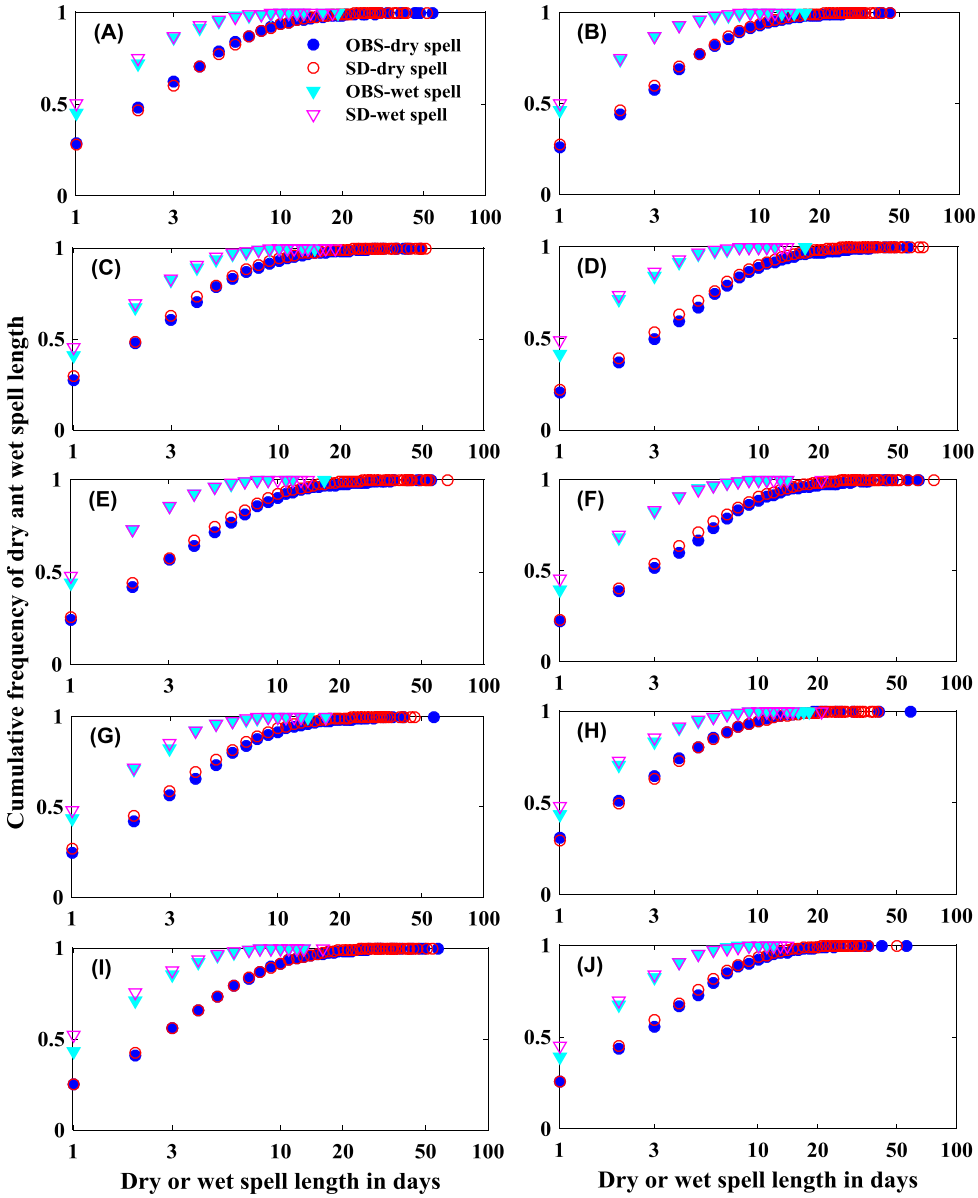

Fig. 8 Observed and downscaled cumulative frequencies of dry and wet spells for the validation period over all 10 stations within the Hanjiang River watershed

percentiles. However, the K–S test shows that the difference between the observed and downscaled distributions are insignificant for all stations at the P = 0.05 level for both monthly and annual precipitation. The distribution of monthly precipitation is better reproduced than that of the annual precipitation, as indicated by the higher P values of the K–S tests.

5 Discussion and conclusion

This study proposed a two-stage multi-site downscaling approach by coupling a single-site downscaling method and a MSWG. The first stage is the spatial downscaling of monthly precipitation from climate model scale to station scale using a quantile mapping method. The quantile mapping method can be classified as a MOS bias correction method. Many studies (e.g. Chen et al. 2013b; Teutschbein and Seibert 2012) have used the quantile mapping method to produce climate change scenarios for impact studies, and it has been proven to be better than mean-based scaling methods. MOS bias correction methods are developed based on a bias stationary assumption. In other words, when using them, the biases of climate model outputs are assumed to be constant between future and reference periods (or between calibration and validation periods). Theoretically, when the biases of a future period are larger than those of the reference period, the bias correction method can improve the climate simulation for the future period. Even when

Table 3 Statistics of observed and downscaled daily precipitation amounts (mm) for the validation period for all ten stations within the Hanjiang River watershed (MDP = maximum daily precipitation, and MWD = mean wet days)

Station	Source	Mean	Stdev	Skewness	Kurtosis	25th	50th	75th	90th	95th	99th	MDP	MWD
S1	OBS	6.4	11.2	4.7	40.8	0.6	2.3	7.5	17.2	26.9	52.8	161.8	126.0
	SD	5.8	8.1	3.4	21.1	0.9	2.9	7.4	14.3	20.9	39.4	106.5	123.2
S2	OBS	7.1	11.7	3.4	19.6	0.6	2.5	8.1	19.8	29.7	56.6	121.4	120.7
	SD	6.3	9.8	3.9	27.2	0.9	2.8	7.6	16.1	24.6	48.7	159.3	123.2
S3	OBS	7.2	12.6	4.6	40.5	0.6	2.5	8.1	20.0	30.7	59.9	203.3	131.3
	SD	6.2	9.4	3.8	26.9	0.9	2.8	7.7	16.0	24.0	45.0	147.1	133.8
S4	OBS	6.7	10.2	3.2	18.4	0.7	2.7	8.2	17.9	27.5	49.0	105.4	105.3
	SD	5.8	7.8	2.9	15.5	1.0	3.0	7.4	14.9	21.2	37.9	89.3	107.9
S5	OBS	6.9	10.7	3.3	20.0	0.7	2.8	8.4	18.7	27.7	51.5	125.1	110.1
	SD	5.9	8.9	3.4	19.3	0.8	2.5	6.9	15.4	23.5	43.5	102.2	117.2
S6	OBS	7.8	13.4	4.5	41.0	0.7	2.7	9.0	21.9	32.5	64.4	217.0	109.6
	SD	7.2	9.6	3.0	17.6	1.3	3.7	9.2	18.5	26.6	45.5	139.7	115.1
S7	OBS	7.4	12.7	3.5	18.6	0.7	2.6	8.2	20.1	32.4	65.0	119.8	118.9
	SD	6.3	10.3	4.0	27.3	0.9	2.5	7.1	16.3	25.3	49.9	156.2	123.6
S8	OBS	9.6	19.9	4.8	36.0	0.5	2.6	9.4	24.6	45.2	94.9	255.8	138.6
	SD	8.3	14.0	3.8	24.0	1.0	3.1	9.3	21.9	34.2	70.6	167.5	131.9
S9	OBS	7.3	11.8	3.0	15.2	0.6	2.5	8.5	21.7	31.4	56.4	113.6	117.0
	SD	6.6	10.0	3.3	19.3	0.8	2.8	8.0	18.0	26.1	48.9	115.4	112.5
S10	OBS	6.8	10.5	3.3	20.0	0.7	2.6	8.2	18.6	28.0	48.9	128.9	124.7
	SD	6.4	8.7	3.1	17.2	1.1	3.3	8.3	16.4	23.2	42.3	103.6	128.1

Table 4 Statistics of observed and downscaled monthly precipitation amounts (mm) for the validation period for all 10 stations within the Hanjiang River watershed (MMP = maximum monthly precipitation)

Station	Source	Mean	Stdev	Skewness	Kurtosis	25th	50th	75th	90th	95th	99th	MMP	K–S test
S1	OBS	62.4	65.8	1.5	5.5	10.4	42.6	93.1	150.6	198.8	296.1	332.2	0.731
	SD	59.1	57.9	1.3	4.4	10.0	41.9	91.4	139.3	175.4	247.9	287.3	
S2	OBS	68.4	66.3	1.4	5.1	15.1	49.1	102.0	158.5	201.3	291.0	370.4	0.437
	SD	65.1	59.7	1.3	5.0	15.9	51.4	94.5	148.2	184.3	259.3	339.1	
S3	OBS	74.7	79.6	1.6	5.8	13.3	51.1	114.3	173.3	242.9	341.1	446.8	0.640
	SD	69.5	64.9	1.2	4.5	14.1	52.7	105.9	159.9	200.8	265.2	426.4	
S4	OBS	56.6	56.7	1.6	6.3	12.8	39.9	82.4	134.5	173.6	267.6	349.0	0.463
	SD	52.3	46.0	1.2	4.7	12.8	44.0	77.9	115.3	142.4	199.6	271.5	
S5	OBS	62.7	64.2	1.6	6.0	12.9	43.8	90.8	158.2	184.8	298.4	344.0	0.584
	SD	57.2	53.2	1.2	4.4	12.1	43.7	87.3	131.9	167.1	216.6	317.4	
S6	OBS	68.5	69.6	1.8	7.8	17.6	46.7	98.6	161.1	208.2	303.5	480.1	0.571
	SD	68.7	64.5	1.4	4.7	18.6	49.3	97.6	163.0	201.5	284.5	332.5	
S7	OBS	71.4	74.7	1.6	5.4	14.9	44.4	102.7	179.2	215.5	338.8	380.2	0.426
	SD	64.5	60.4	1.3	4.3	15.1	49.8	95.6	149.7	183.8	261.4	326.0	
S8	OBS	103.6	113.3	1.7	6.5	15.4	64.4	161.1	253.5	341.1	464.8	730.7	0.241
	SD	99.7	91.2	1.4	5.2	13.8	66.0	138.7	218.0	270.7	376.0	561.7	
S9	OBS	67.1	67.9	1.7	7.7	14.1	47.3	100.6	147.9	186.8	287.3	455.0	0.802
	SD	61.9	57.9	1.2	4.5	12.3	46.8	95.7	143.7	171.0	236.1	368.8	
S10	OBS	68.0	60.1	1.3	5.7	18.0	50.4	107.8	150.5	179.8	223.4	414.6	0.571
	SD	68.7	57.0	0.9	3.7	18.3	56.7	105.7	147.1	175.4	225.7	342.5	

the biases of a future period are smaller than those of the reference period, the bias correction method may still have beneficial effects. Only when the future period biases are reduced to less than half of the reference biases will the bias correction method deteriorate the original future simulations (Maraun 2012). A recent study (Chen

Table 5 Statistics of observed and downscaled annual precipitation amounts (mm) for the validation period for all 10 stations within the Hanjiang River watershed (MAP = maximum annual precipitation)

Station	Source	Mean	Stdev	Skewness	Kurtosis	25th	50th	75th	90th	95th	99th	MAP	K–S test
S1	OBS	749.3	131.9	0.1	2.2	650.8	721.0	854.2	903.5	997.5	1001.1	1001.1	0.061
	SD	709.6	114.9	0.3	3.3	638.9	704.2	789.3	853.0	896.9	1022.7	1031.9	
S2	OBS	820.6	179.3	0.5	3.4	720.5	809.5	904.0	1049.0	1147.4	1298.1	1298.1	0.419
	SD	781.7	127.4	0.4	3.1	687.5	779.5	853.0	962.6	1009.1	1139.1	1157.9	
S3	OBS	896.9	155.7	0.3	2.4	771.0	894.4	1017.4	1115.4	1178.6	1222.6	1222.6	0.199
	SD	833.7	128.8	-0.1	3.2	733.1	848.8	912.1	991.9	1039.6	1144.9	1175.5	
S4	OBS	679.3	142.0	0.1	2.4	585.5	667.9	773.4	901.8	918.8	950.5	950.5	0.106
	SD	627.1	96.2	0.0	2.5	553.7	631.9	700.7	747.8	780.6	855.8	870.3	
S5	OBS	752.0	145.6	0.7	3.4	659.8	732.2	829.7	952.9	1022.3	1146.0	1146.0	0.106
	SD	685.8	108.8	0.2	2.5	597.5	686.2	768.8	827.3	869.9	945.4	957.7	
S6	OBS	822.2	149.0	0.9	2.7	720.6	762.4	939.2	1082.9	1130.5	1157.0	1157.0	0.129
	SD	824.1	140.9	0.2	2.6	725.6	815.1	918.6	1020.9	1071.3	1149.9	1161.8	
S7	OBS	856.5	170.4	0.6	2.7	738.7	834.2	928.6	1145.3	1173.1	1240.4	1240.4	0.073
	SD	773.4	118.5	-0.1	2.5	688.2	777.1	867.3	904.3	967.8	1029.3	1053.1	
S8	OBS	1243.6	240.4	0.4	2.5	1064.2	1182.3	1415.7	1613.0	1687.3	1767.3	1767.3	0.137
	SD	1196.7	172.3	0.2	2.4	972.5	1091.9	1196.7	1335.8	1398.6	1478.8	1487.1	
S9	OBS	805.1	164.1	0.7	3.1	673.3	793.8	891.9	1049.3	1085.0	1231.9	1231.9	0.117
	SD	742.8	136.7	0.4	2.6	635.5	737.8	822.0	933.7	992.5	1071.2	1093.6	
S10	OBS	815.8	155.5	0.6	3.1	720.1	802.8	881.9	1035.6	1158.2	1176.6	1176.6	0.439
	SD	824.5	109.6	0.1	2.5	752.6	809.9	897.6	973.1	1013.5	1066.3	1087.2	

et al. 2015b) showed that the precipitation bias is non-stationary, even over two continuous historical periods. To understand the results more clearly, the assumption of bias stationarity is also verified for all 10 stations within the Hanjiang River watershed. Figure 9 presents the difference in biases between the calibration and validation periods for NCEP (Fig. 9a) and downscaled (Fig. 9b) mean annual precipitation. The bias is defined as the percent difference of the mean annual precipitation between the observed and the NCEP (or downscaled) data. The results show that the bias of mean annual precipitation is not stationary, as indicated by the difference in biases between the calibration and validation periods (Fig. 9a). After bias correction, the difference in biases remains for the validation period (Fig. 9b), even though the quantile mapping method shows significant effects on reducing biases for both calibration and validation periods (results not shown). In order to remove the potential effects of interannual variations to a certain extent, this study defines the calibration and validation periods as the odd and even years, respectively. When using the quantile mapping method for a future period, its performance

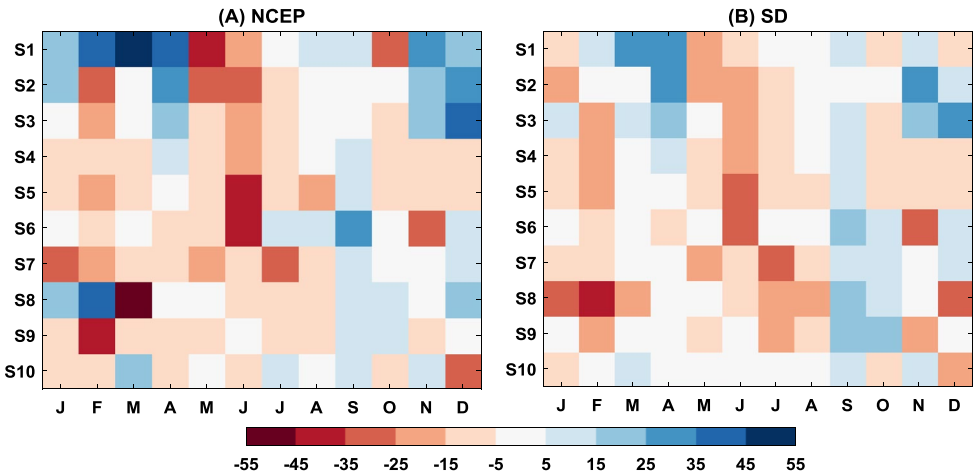

Fig. 9 Difference in bias (%) of mean annual precipitation between calibration and validation periods without (**a**) and with (**b**) spatial downscaling (S1 to S10 represent ten stations within the Hanjiang River watershed)

may be deteriorated, due to the bias non-stationarity. This aspect needs to be further tested in future studies.

In the second stage, monthly precipitation simulations are temporally downscaled to daily scale using a MSWG. One of the most difficult steps in the temporal downscaling of precipitation is to downscale precipitation occurrence. Since downscaling of precipitation occurrence is achieved by linking mean monthly precipitation to probabilities of precipitation occurrence, the performance depends on these relationships. These relationships have been verified in several studies using long time series that have proven the existence of strong correlations (e.g. Zhang et al. 2012; Zhang 2013; Chen et al. 2014c). Even though those earlier studies showed that a period longer than 30 years is necessary for calculating the probabilities of precipitation occurrence to obtain reliable linear relationships, the use of 15 years (the 30-year calibration period was separated into two groups for calculating probabilities) in this study seems to be adequate for this watershed. This shorter time period is exceptionally valid for this watershed in large part because its wet and dry statuses are evenly distributed for precipitation time series. The above downscaling method for precipitation occurrence is based on an assumption that the fitted linear relationships are valid for the future period. In fact, including the two endpoints (wet and dry groups) for establishing the linear relationship, implicitly incorporating non-stationary climate states, is adequate for regressing P01 and P11 for any climatic conditions within the entire range (Zhang 2013). In other words, when using the two endpoints, the non-stationary precipitation should not have an effect on the estimated P01 and P11.

With the reliable transition probabilities and mean monthly precipitation, the mean daily precipitation is obtained using analytical relationships (Eqs. (4)–(6)). The change in mean daily precipitation is then used to adjust the OI curves. Thus, the downscaled daily precipitation also relies on the relationship between daily mean precipitation and the OI. A strong relationship between those two values has been found in other studies (e.g. Brissette et al. 2007; Chen et al. 2014c). To remove the noise of the calculated mean precipitation, attributed to the short time series (especially at the monthly basis), a monotonic curve is fitted. Because of the deviation between the fitted curve and the real values, the generated mean daily precipitation may not be identical to that calculated using analytical equations. The adjustment of the OI curves assumes that the dependency of mean precipitation and OI will be valid for the future period. From the OI definition, it is understood that the correlation of occurrence vector is a weighting function that takes into account the fact that an occurrence at a station with high correlations is more significant than one at a station with low correlations. Even though a weight vector may be defined based on other metrics, such as station distance and topography, the use of observed correlation coefficients makes sense since they are physically-based and readily available (Brissette et al. 2007). The historical correlations of precipitation occurrence have been tested and found to be unchanged in the future period; and thus the dependency of mean precipitation and OI would also be valid for non-stationary precipitation conditions.

The overall performance of the downscaled precipitation time series depends on the abilities of the above three aspects (quantile mapping downscaling, downscaling precipitation occurrence and the OI relationship). The generated daily precipitation is compared to observed data using the cumulative frequencies of wet and dry spells and statistics of precipitation amounts at daily, monthly and annual scales as criteria. Since each of the above three aspects can introduce biases to the final results, the daily precipitation is not accurately reproduced. However, the statistics of monthly and annual precipitation are reasonably reproduced for most stations, which reflect the good overall performance of the proposed downscaling approach.

The proposed downscaling approach has a few advantages compared to other methods. (1) Since it is based on a MSWG, the inter-station correlation is accurately preserved, and thus can be used to investigate the spatial variability of climate change impacts. (2) It uses monthly precipitation as the predictor for spatial downscaling. Previous studies (e.g. Maurer and Hidalgo 2008) have shown that climate models tend to be more accurate and reliable when simulating monthly precipitation rather than daily values. In addition, monthly precipitation is more readily available than daily precipitation. (3) Precipitation occurrence is specifically downscaled. Other statistical downscaling methods (e.g. the regression-based PP method and the MOS bias correction method) may also consider precipitation occurrence. However, regression methods usually poorly reproduce the observed precipitation occurrence, due to the lack of a strong relationship between precipitation occurrence and large-scale climate variables (Chen et al. 2012a, 2014a). Additionally, the MOS bias correction methods only consider the wet-day frequency, and ignore the temporal structure (sequence) of precipitation occurrence (Chen et al. 2013b). (4) The proposed method estimates the relationship between the observed monthly precipitation and its climate model counterpart, which circumvents the weak relationship between observed daily precipitation and large-scale climate variables encountered when using PP methods (Chen et al. 2012a, 2014a). (5) The proposed method is suitable for downscaling precipitation for both stationary and non-stationary climate conditions (Mullan et al. 2016), as the disaggregation process involves adjusting the parameters of a parametric distribution. This parameter adjustment results in a new distribution for non-stationary conditions.

Overall, a multi-site downscaling approach coupling a single-site downscaling method and a MSWG is proposed here. This method offers a satisfactory performance and is efficient in generating multi-site climate change scenarios for studying the spatial variability of climate change impacts on hydrology. Due to data availability, the method is only evaluated for one large watershed in China. Since the relationships involved in this downscaling approach may be spatially- and temporally-dependent, additional evaluations may be needed when using this approach for new regions.

Acknowledgements This work was partially supported by the Key Programs of the National Natural Science Foundation of China (Grant Nos. 51539009, 51339004), the Thousand Youth Talents Plan from the Organization Department of CCP Central Committee (Wuhan University, China). The authors would like to acknowledge the NOAA/OAR/ESRL PSD (http://www.esrl.noaa.gov/psd/), Boulder, Colorado, USA for providing NCEP reanalysis precipitation. The authors wish to thank the China Meteorological Data Sharing Service System and the Bureau of Hydrology of the Changjiang Water Resources Commission for providing the dataset for the Hanjiang River watershed.

References

Baigorria GA, Jones JW (2010) GiST: a stochastic model for generating spatially and temporally correlated daily rainfall data. J Clim 23(22):5990–6008

Brissette FP, Khalili M, Leconte R (2007) Efficient stochastic generation of multi-site synthetic precipitation data. J Hydrol 345(3–4):121–133

Chen J, Brissette FP (2014a) Comparison of five stochastic weather generators in simulating daily precipitation and temperature for the Loess Plateau of China. Int J Climatol 34:3089–3105

Chen J, Brissette FP (2014b) Stochastic generation of daily precipitation amounts: review and evaluation of different models. Clim Res 59:189–206

Chen J, Brissette FP, Chaumont D, Braun M (2013a) Performance and uncertainty evaluation of empirical downscaling methods in quantifying the climate change impacts on hydrology over two North American river basins. J Hydrol 479:200–214

Chen J, Brissette FP, Chaumont D, Braun M (2013b) Finding appropriate bias correction methods in downscaling precipitation for hydrologic impact studies over North America. Water Resour Res 49:4187–4205

Chen J, Brissette F, Leconte R (2010) A daily stochastic weather generator for preserving low-frequency of climate variability. J Hydrol 388:480–490

Chen J, Brissette FP, Leconte R (2011b) Assessment and improvement of stochastic weather generators in simulating maximum and minimum temperatures. Trans ASABE 54(5):1627–1637

Chen J, Brissette FP, Leconte R (2011a) Uncertainty of downscaling method in quantifying the impact of climate change on hydrology. J Hydrol 401:190–202

Chen J, Brissette FP, Leconte R (2012a) Coupling statistical and dynamical methods for spatial downscaling of precipitation. Clim Change 114:509–526

Chen J, Brissette FP, Leconte R (2012b) Downscaling of weather generator parameters to quantify the hydrological impacts of climate change. Clim Res 51(3):185–200

Chen J, Brissette FP, Leconte R (2014a) Assessing regression-based statistical approaches for downscaling precipitation over North America. Hydrol Process 28:3482–3504

Chen J, Brissette FP, Leconte R, Caron A (2012c) A versatile weather generator for daily precipitation and temperature. Trans ASABE 55(3):895–906

Chen J, Brissette F, Lucas-Picher P (2015a) Assessing the limits of bias correcting climate model outputs for climate change impact studies. J Geophys Res Atmos 120(3):1123–1136

Chen J, Brissette FP, Zhang XC (2014b) A multi-site stochastic weather generator for daily precipitation and temperature. Trans ASABE 57(5):1375–1391

Chen J, Brissette FP, Zhang XC (2015b) Hydrological modeling using a multi-site stochastic weather generator. J Hydrol Eng. doi:10.1061/(ASCE)HE.1943-5584.0001288

Chen J, Zhang XC, Liu WZ, Li Z (2009) Evaluating and extending CLIGEN precipitation generation for the Loess Plateau of China. JAWRA 45(2):378–396

Chen J, St-Denis BG, Brissette FP, Lucas-Picher P (2016) Using natural variability as a baseline to evaluate the performance of bias correction methods in hydrological climate change impact studies. J Hydrometeorol 17(8):2155–2174

Chen J, Zhang XC, Brissette FP (2014c) Assessing scale effects for statistically downscaling precipitation with GPCC model. Int J Climatol 34:708–727

Christensen JH, Boberg F, Christensen OB, Lucas-Picher P (2008) On the need for bias correction of regional climate change projections of temperature and precipitation. Geophys Res Lett 35:L20709. doi:10.1029/2008GL035694

Dickinson RE, Errico RM, Giorgi F et al (1989) A regional climate model for the western United-States. Clim Change 15(3):383–422

Dubrovsky M, Buchteke J, Zalud Z (2004) High-frequency and low-frequency variability in stochastic daily weather generator and its effect on agricultural and hydrologic modeling. Clim Change 63:145–179

Giorgi F (1990) Simulation of regional climate using a limited area model nested in a general-circulation model. J Clim 3(9):941–963

Guo Y, Senior MJ (2006) Climate model simulation of point rainfall frequency characteristics. J Hydrol Eng. doi:10.1061/(ASCE)1084-0699

Herrera S, Fita L, Fernandez J, Gutierrez JM (2010) Evaluation of the mean and extreme precipitation regimes from the ENSEMBLES regional climate multimodel simulations over Spain. J Geophys Res. doi:10.1029/2010JD013936

Huang JC, Yu CK, Lee JY, Cheng LW, Lee TY, Kao SJ (2012) Linking typhoon tracks and spatial rainfall patterns for improving flood lead time predictions over a mesoscale mountainous watershed. Water Resour Res 48:W09540. doi:10.1029/2011WR011508

Iman RL, Conover WJ (1982) A distribution-free approach to inducing rank correlation among input variables. Comm. Statistics B11(3):311–334

Ines AVM, Hansen JW (2006) Bias correction of daily GCM rainfall for crop simulation studies. Agric For Meteor 138: 44–53

Johnson F, Sharma A (2012) A nesting model for bias correction of variability at multiple time scales in general circulation model precipitation simulations. Water Resour Res 48:W01504. doi:10.1029/2011WR010464

Kalnay E, Kanamitsu M, Kistler R, Collins W, Deaven D, Gandin L, Iredell M, Saha S, White G, Woollen J, Zhu Y, Leetmaa A, Reynolds R, Chelliah M, Ebisuzaki W, Higgins W, Janowiak J, Mo KC, Ropelewski C, Wang J, Jenne R, Joseph D (1996). The NCEP/NCAR 40-Year Reanalysis Project. B Am Meteorol Soc 77:437–471

Li Z (2013) A new framework for multi-site weather generator: A two-stage model combining a parametric method with a distribution-free shuffle procedure. Clim Dyn 43(3–4):657–669

Li Z, Liu WZ, Zhang XC, Zheng FL (2011) Assessing the site-specific impacts of climate change on hydrology, soil erosion and crop yields in the Loess Plateau of China. Clim Change 105(1):223–242

Maraun D (2012) Nonstationarities of regional climate model biases in European seasonal mean temperature and precipitation sums. Geophys Res Lett 39(6):70–82

Maraun D, Wetterhall F, Ireson AM, Chandler RE, Kendon EJ, Widmann M, Brienen S, Rust HW, Sauter T, Themeßl M, Venema VKC, Chun KP, Goodess CM, Jones RG, Onof C, Vrac M, Thiele-Eich I (2010) Precipitation downscaling under climate change: recent developments to bridge the gap between dynamical models and the end user. Rev Geophys 48(3):RG3003 8755–1209

Maurer EP, Hidalgo HG (2008) Utility of daily vs. monthly largescale climate data: an intercomparison of two statistical downscaling methods. Hydrol Earth Syst Sci 4:3413–3440

Mpelasoka FS, Chiew FHS (2009) Influence of rainfall scenario construction methods on runoff projections. J Hydrometeor 10:1168–1183

Mullan D, Chen J, Zhang XC (2016) Validation of non-stationary precipitation series for site-specific impact assessment: comparison of two statistical downscaling techniques. Clim Dyn 46:967–986

Piani C, Haerter O, Corpola E (2010) Statistical bias correction for daily precipitation in regional climate models over Europe. Theor Appl Climatol 99:187–192

Qian BD, Gameda S, Jong R, Fallon P, Gornall J (2010) Comparing scenarios of Canadian daily climate extremes derived using a weather generator. Clim Res 41(2):131–149

Qian BD, Hayhoe H, Gameda S (2005) Evaluation of the stochastic weather generators LARS-WG and AAFC-WG for climate change impact studies. Clim Res 29:3–21

Richardson CW (1981) Stochastic simulation of daily precipitation, temperature, and solar radiation. Water Resour Res 17(1):182–190

van Roosmalen L, Christensen JH, Butts MB, Jensen KH, Refsgaard JC (2010) An intercomparison of regional climate model data for hydrological impact studies in Denmark. J Hydrol 380:406–419

Rosenberg EA, Keys PW, Booth DB, Harley D, Burkey J, Steinemann AC, Lettenmaier DP (2010) Precipitation extremes and the impacts of climate change on stormwater infrastructure in Washington State. Clim Change 102:319–349

Semenov MA (2007) Development of high-resolution UKCIP02-based climate change scenarios in the UK. Agric For Meteor 144:127–138

Smith JA, Miller AJ, Baeck ML, Nelson PA, Fisher GT, Meierdiercks KL (2005) Extraordinary flood response of a small urban watershed to short-duration convective rainfall. J Hydrometeorol 6(5):599–617

Teutschbein C, Seibert J (2012) Bias correction of regional climate model simulations for hydrological climate-change impact studies: review and evaluation of different methods. J Hydrol 456–457:12–29

Themeßl MJ, Gobiet A, Leuprecht A (2010) Empirical statistical downscaling and error correction of daily precipitation from regional climate models. Int J Climatol. doi:10.1002/joc.2168

Themeßl MJ, Gobiet A, Heinrich G (2012) Empirical-statistical downscaling and error correction of regional climate models and its impact on the climate change signal. Clim Change 112:449–468

Themeßl MJ, Gobiet A, Leuprecht A (2011) Empirical-statistical downscaling and error correction of daily precipitation from regional climate models. Int J Climatol 31:1530–1544

Thiele-Eich L (2010) Precipitation downscaling under climate change. Recent developments to bridge the gap between dynamical models and the end user. Rev Geophys. doi:10.1029/2009RG000314

Wang QJ, Nathan RJ (2007) A method for coupling daily and monthly time scales in stochastic generation of rainfall series. J Hydrol 346:122–130

Wilby RL, Conway D, Jones PD (2002b) Prospects for downscaling seasonal precipitation variability using conditioned weather generator parameters. Hydrol Process 16:1215–1234

Wilby RL, Dawson CW, Barrow EM (2002a) SDSM—a decision support tool for the assessment of regional climate change impacts. Environ Modell Softw 17:145–157

Wilks DS (1992) Adapting stochastic weather generation algorithms for climate change studies. Clim Change 22:67–84

Wilks DS (1998) Multisite generalization of a daily stochastic precipitation generation model. J Hydrol 210(1–4):178–191

Wilks DS (1999) Multisite downscaling of daily precipitation with a stochastic weather generator. Clim Res 11:125–136

Wilks DS (2010) Use of stochastic weather generator for precipitation downscaling. WIREs. Clim Change 1:898–907

Yang W, Andreasson J, Graham LP, et al (2010) Distribution-based scaling to improve usability of regional climate model projections for hydrological climate change impacts studies. Hydrol Res 41(3–4):211–229

Zhang XC (2005a) Spatial downscaling of global climate model output for site-specific assessment of crop production and soil erosion. Agric For Meteor 135:215–229

Zhang XC (2005b) Generation correlative storm variables for CLIGEN using a distribution-free approach. Trans ASAE 48(2):567–575

Zhang XC (2013) Verifying a temporal disaggregation method for generating daily precipitation of potentially non-stationary climate change for site-specific impact assessment. Int J Climatol 33:326–342

Zhang XC, Chen J, Garbrecht JD, Brissette FP (2012) Evaluation of a weather generator-based method for statistically downscaling nonstationary climate scenarios for impact assessment at a point scale. Trans ASABE 55(5):1745–1756

Zhang XC, Liu WZ, Li Z, Chen J (2011) Trend and uncertainty analysis of simulated climate change impacts with multiple GCMs and emission scenarios. Agric For Meteor 151(10):1297–1304